Proceedings of the Seventh International Conference on
Railway Technology: Research, Development and Maintenance
Edited by: J. Pombo
Civil-Comp Conferences, Volume 15, Paper 17.7
Civil-Comp Press, Edinburgh, United Kingdom, 2026
ISSN: 2753-3239, doi: 10.4203/ccc.15.17.7

A Mechanico-Statistical Approach for the Assessment of Broken Rail Prevention on the Grand Paris Express

B. Laurent[1], O. François[1], A. Panunzio[2], S. Simon[2], M. Essadeq[3], D. Drago[3], F. Parrennes[4] and M. Cogne[5]

[1]Gustave Eiffel University, COSYS-GRETTIA, Champs sur Marne, France
[2]IMDM Group, Paris, France
[3]Systra, Saint Denis, France
[4]RATP, La Pleine Daint Denis, France
[5]Société des Grands Projets, Saint Denis, France

Abstract

Broken rail prevention is a major challenge for any railway infrastructure manager. It requires the definition of a consistent and rational strategy for rail inspection and preventive maintenance. The determination of optimal parameters is often facilitated by the implementation of digital twins, which make it possible to evaluate the behaviour of decision indicators under different inspection and maintenance configurations. These maintenance strategy assessment tools are generally based on operational feedback data, allowing the dynamics of defect initiation and propagation to be characterized in various contexts. In the case of the future Grand Paris Express, no such data are available, as no network of comparable scale and operating conditions has yet been operated. To overcome this limitation, this paper proposes a mechanico-statistical approach for initializing rail lifetime parameters under different contexts and subsequently running simulations for various operating, inspection, and maintenance parameter sets, relying on the generic VirMaLab virtual maintenance laboratory framework based on Bayesian network formalism.

Keywords: railway maintenance, broken rail prevention, predictive maintenance, maintenance optimisation, statistical modelling, mechanical modelling, Bayesian networks, decision support.

1 Introduction

In 2010, the French government presented its roadmap for the development of a new metro network featuring rapid transit lines in the Île-de-France region, aimed at

addressing the saturation of the existing network—particularly along the East–West and North–South corridors—and at connecting the region's major residential, higher education, and employment hubs. The Grand Paris Express (GPE) thus became the largest transport project in Europe. It represents a fundamental reorganization of mobility in the Paris region, with new lines enabling rapid circumferential travel around Greater Paris without having to pass through the city centre, as required by the current star-shaped network structure. This new network is markedly different from those found elsewhere in the world. To date, no other network is equivalent to what the GPE will become (with the possible exception of Dubai's Red Line, for which no significant feedback data are available). Without track circuits or drivers, and with high service frequencies and operating speeds, the detection and prevention of rail breaks have become major challenges. In most cases, feedback data are used to understand the dynamics of defect initiation and propagation leading to rail failures and, consequently, to define the performance requirements and inspection frequencies of monitoring systems needed to meet operational and safety objectives.
In 2015, an initial project was launched involving the former IFSTTAR (now Université Gustave Eiffel), the Société du Grand Paris (now Société des Grands Projets), and the RATP to develop a decision-support tool for assessing rail break risks and determining the required characteristics of inspection systems to ensure safe operations (Bouillaut et al., 2020).
Ten years later, as the inauguration of the first lines approaches, the various stakeholders of this new network continue work on tools and technologies to ensure that the safety, availability, and service quality objectives of these new lines are met. The study presented in this paper is part of this context. In the case of the GPE, no similar network currently exists (or at least no significant operational feedback is available). Standard approaches, based on statistical analysis, could therefore not be directly implemented, as was previously done using the generic VirMaLab framework. To address this issue, a mechanico-statistical approach was proposed.

The remainder of this paper is organized as follows. First, the general context of the study is introduced. Sections 3 and 4 then present, respectively, the VirMaLab generic formalism and the proposed mechanico-statistical approach. Finally, before the conclusions and perspectives, Section 5 focuses on some illustrative results to highlight the feasibility of our method and its relevance for infrastructure managers.

2 The "Grand Paris Express" Project Context

The Grand Paris Express (GPE) is a large-scale public transport project aimed at creating an automated metro network connecting the suburbs of the Paris region both to each other and to the centre of the capital. Launched in 2010, this ambitious project is expected to be fully completed by 2030. It is the largest urban transport project in Europe. Today, the metro and RER systems form a star-shaped network with Paris at its centre. The Grand Paris Express is a new automated steel-wheel metro system (driverless and without rubber tires) that will connect the region's main residential and activity hubs directly to one another—without passing through Paris—particularly major strategic regional centres and previously underserved metropolitan areas, as illustrated in Figure 1.

Figure 1: Structure of the future GPE network, looking ahead to 2030.

The primary objective of the Grand Paris Express is to relieve congestion on roads and existing public transport networks, which are often saturated and inefficient, by offering a faster and more reliable transportation alternative. The network will include four new lines—Lines 15, 16, 17, and 18—totalling approximately 220 kilometres of track, including more than 140 km in tunnels and over 68 new stations, serving the most densely populated areas of the Paris region.
The project is also designed to stimulate economic and urban development in previously underserved suburban areas. By creating new economic, cultural, and residential hubs around metro stations, the Grand Paris Express is viewed as a key component of the region's strategy for economic development and social cohesion.
Overall, the GPE is a major project expected to have a significant impact on the daily lives of residents in the Paris region, as well as on its economy and urban development. It represents a substantial step forward in improving connectivity, reducing congestion, and enhancing quality of life for millions of people.
The GPE project also stands out for its major technological innovations in the railway sector. It constitutes the first European implementation of an automated steel-wheel metro system without track circuits (TC). This feature raises a critical issue in terms of track maintenance, particularly regarding the detection of sudden transverse rail breaks—a defect historically detected in part by track circuits, in addition to inspection campaigns and on-site maintenance patrols. Although track circuits are not designed to safely detect such failures, operational feedback shows that they have often served as an ultimate detection layer within the safety culture of existing networks.
Given this criticality, the GPE reinforces the need for a more efficient and optimized maintenance strategy. To this end, the infrastructure manager (RATP GI) will be

equipped with a comprehensive set of advanced inspection systems aimed at improving track maintenance control. These inspection vehicles—capable of operating either within the passenger train rotation schedule (outside peak hours) or during non-operational periods-include:

- Ultrasonic measurement systems for internal rail inspection.
- An on-board video monitoring system for assessing track surface condition.

In addition, all passenger rolling stock will be equipped with onboard accelerometer-based monitoring systems dedicated to the early detection of major rail defects. This large-scale innovative system will complement the preventive maintenance strategy. Together, these devices are part of a condition-based and predictive maintenance approach, which is essential to ensuring the safety and availability of the new automated network.

Since 2025, the *Société des Grands Projets* (SGP), supported by SYSTRA and the infrastructure manager, has been collaborating with *Université Gustave Eiffel* (UGE) to develop tools aimed at optimizing inspection frequencies. The objective is to detect small defects, monitor their growth over time, and enable the planning of preventive maintenance actions before a defect evolves into a "broken rail." The methodology, called VirMaLab (introduced in Section III), contributes to the process of optimizing inspection frequencies.

3 VirMaLab Virtual Maintenance Laboratory

The increasing complexity of industrial systems and the growing requirements in terms of availability—driven by competitiveness and productivity needs—have made maintenance optimization a key issue both during operation and at the design stage. At the same time, stakeholders in the railway sector have witnessed major advances in measurement, transmission, storage, and data analysis technologies. These developments have enabled new ways of exploiting feedback data collected from infrastructure inspection campaigns and rolling stock instrumentation. Since the early 2000s, railway stakeholders have therefore sought to improve their maintenance strategies, which had until then largely been based on a compromise—more or less optimal and often empirically defined—between corrective actions and systematic preventive maintenance.

To address these needs, a generic approach was proposed for developing decision-support tools capable of determining optimal maintenance, operation, and monitoring parameters. This methodology, called VirMaLab (Virtual Maintenance Laboratory), relies on block-based modelling using probabilistic graphical models (Bayesian networks). Initially introduced in the doctoral work of Roland Donat (Donat, 2009) and later extended through various railway applications (Bouillaut et al., 2011), these tools address multi-component systems, potentially interacting, with finite and discrete states.

Figure 2 presents the generic graphical structure of the Bayesian network adopted in the implementation of a VirMaLab-type decision-support tool (this structure can, of course, be adapted depending on the specific system under consideration). It includes three main blocks modelling respectively the degradation process, the inspection chain and maintenance actions, and the evaluation parameters of a given strategy.

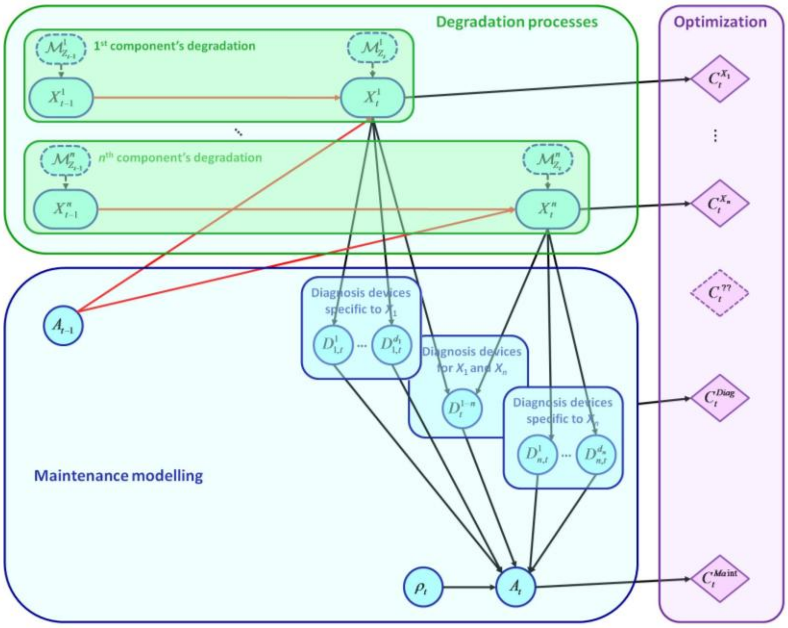

Figure 2: Graphical structure of the Dynamic Bayesian Network used to develop a VirMaLab-type decision-support tool.

In this framework, each component has its own degradation model. The variable X^i represents the state of the i^{th} component at time t. To reflect real-world situations as closely as possible, modelling is based on probabilistic graphical models (PGMs) (Donat et al., 2009). This specific Bayesian network structure allows modelling the dwell time in each state for every component according to arbitrary probability distributions - generally learned from feedback data or elicited from expert advices - thus avoiding the classical Markovian assumption, which is often too restrictive for industrial applications. Each degradation model $X^i(t)$ may also be influenced by contextual variables (nodes Z^i). Furthermore, interactions between degradation processes of different components can be incorporated (the state of component i may influence the degradation of component j). This is achieved by adding an arc between nodes X^i_{t-1} and X^j_t. However, for the sake of clarity and readability, components are considered independent in Figure 2.

The second block focuses on modelling the diagnostic actors responsible for assessing the condition of the considered components, represented by the set of nodes D. As shown in Figure 2, inspection equipment may be either shared among multiple components or dedicated to a single component. These systems may operate continuously or intermittently (activation controlled by variables δ). Depending on the project and the implemented inspection strategy, a decision-fusion node Δ may also be introduced to combine the outputs of all diagnostic systems contributing to the assessment. These outputs may be weighted according to the level of confidence assigned to each monitoring system. Each diagnostic device D is therefore characterized by its frame of discernment (what it is able to “see”) and by a confusion matrix describing its true detection and misclassification rates. Finally, one (or more) maintenance decision variable(s), denoted a, determines the action to be carried out based on the observed states of each component.

The ultimate objective of VirMaLab is to evaluate, compare, or optimize different maintenance strategies according to user-defined criteria (availability, safety, costs, etc.). The final part of the modelling therefore consists in integrating a set of utilities characterizing system operation, diagnostic actors, and maintenance actions.
At each time *t*, each of these variables may generate utilities (nodes denoted *C*). Although these utilities often correspond to costs (or profits), they may represent any quantity computable from the distribution of the considered random vector. Utilities may thus account for the number of corrective maintenance actions, the number of false alarms, or the frequency with which the system is in a given state, among others. For each defined utility, a specific node is added to the VirMaLab structure, forming an influence diagram that enables evaluation of a given strategy. Unlike other nodes in a probabilistic graphical model, utility nodes are not associated with random variables; they serve solely to specify the variables on which utility calculations are performed.
For further details on the VirMaLab approach (formalism, learning and inference algorithms, previous railway applications, etc.), the reader may refer in particular to Bouillaut et al. (2011) and Bouillaut et al. (2013).

4 A Mechanico-Statistical Approach to Compensate for the Lack of Feedback Data

In any statistical modelling process, a key step lies in calibrating the proposed model so that its behaviour closely matches that of the system under study. When feedback data are available, statistical model parameters are commonly estimated using maximum likelihood (or other learning algorithms). However, as introduced in the previous sections, the Grand Paris Express (GPE) is a unique network for which no operational learning data are currently available.
To overcome this limitation, a first mechanico-statistical approach was proposed in a preliminary study in 2020 (Bouillaut et al., 2020). For the VirMaLab–GPE project presented in this paper, a revised version of this mechanico-statistical approach was developed and is detailed in the remainder of this section.

4.1. General Principles of the Mechanico-Statistical Approach

Figure 3 presents the general principle of the proposed methodology, which consists of three main steps.
The first step involves leveraging existing knowledge of the technical characteristics of a reference line (for which feedback data were available) and of the GPE line under study. Based on fracture mechanics principles, "mechanical" models developed for both lines allow estimation of the dwell times of homogeneous rail sections (same curvature, rail type, axle load, annual traffic load, track layout, operating speed, and track stiffness) in each of the three rail states preceding failure -according to the International Union of Railways (UIC) classification: OK (no defect observable by inspection systems), X_1 (internal defect between 1.5 mm and 20 mm), X_2 (crack between 20 mm and 30 mm).
More specifically, the evolution of a defect (in plain rail or in a weld), successively subjected to the physical context of the reference line (RER line B for results

introduced in this paper) and then to that of the considered GPE line (in this paper, Line 15 south), is computed.

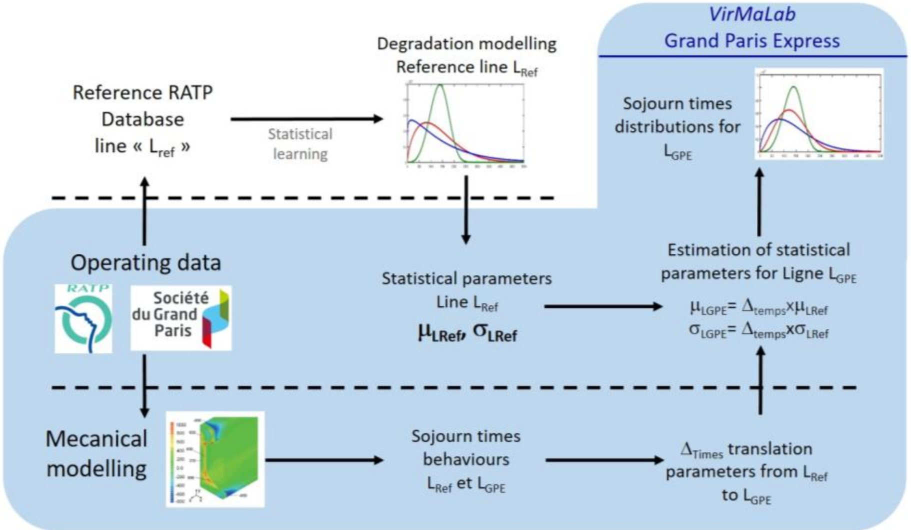

Figure 3: The mechanic-statistical approach proposed for the GPE project.

The rail network of each line is divided into homogeneous sections according to technical characteristics. For each line, this results in a table listing homogeneous section types and their corresponding rail lengths. For each homogeneous section, “local” dwell times in states OK, X_1, and X_2 are simulated for various defect initiation depths ranging from 1.5 mm to 50 mm below the rail surface. “Global” dwell times for the entire line are then obtained by averaging the local dwell times of all homogeneous sections, weighted by: their relative lengths, and the probability of defect initiation as a function of depth (estimated from the degradation history of the reference line). Since RATP historical data showed that dwell times are strongly correlated with horizontal curvature, this analysis was performed by grouping sections according to curvature radius classes: less than 400m, between 400m and 750m, more than 750m and infinite curve (i.e. in alignment tracks sections). Each mechanical model provides parameters for three dwell time distributions (OK, X_1, X_2) for each curvature class. Statistical comparison of these distributions between the reference line and the GPE line yields a “transfer factor” from the reference line to the GPE line.
The second step involves using feedback from the reference line to estimate the parameters of the Weibull distributions that characterize the dwell time in each state and for each context (curve, alignment).
Finally, applying the transfer factors defined earlier to the Weibull distributions calculated in step 2 allows us to define what the observed dwell time distributions on the GPE line “should” be.

4.2. Mechanical Modelling of the Railway Track

As briefly introduced above, the physical model is based on structural mechanics and fracture mechanics principles. Structural mechanics addresses the behaviour of structural elements subjected to loads, including internal forces and deformations. Fracture mechanics studies crack growth in structural elements subjected to cyclic

loading. A load cycle corresponds to the complete loading and unloading process of a structural element under dynamic load. At a given point, it represents the variation of stress from zero to an extremum (either tensile or compressive). Tensile cycles contribute to crack propagation.
For example, Figure 4 schematically illustrates the three main load cycles affecting a crack located in the rail head of a tangent track during axle passage. The rail is modelled as a beam supported by sleepers. When the wheel reaches the adjacent span to the defect location, it induces a positive bending moment (upward curvature) at the defect, generating tensile stress. This stress increases until the wheel reaches mid-span and then decreases to zero at the next sleeper—constituting the first load cycle.

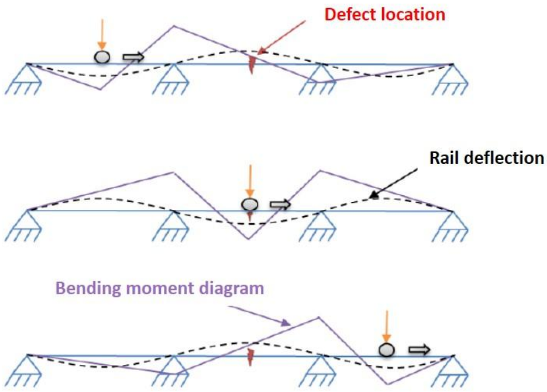

Figure 4: Schematic representation of the three key loading cycles to which a crack located in the head of a rail in a track is subjected

As the wheel moves to the next span, the opposite effect occurs: the defect experiences compressive stresses due to negative bending (downward curvature). These stresses increase until mid-span and decrease back to zero at the following sleeper. Additionally, horizontal shear stresses associated with Hertzian contact (rolling pressure) act radially around the rail-wheel contact surface. Locally, these are comparable to high-intensity tensile stresses (Lefèvre, 1975), so the resulting stresses remain tensile. A third cycle similar to the first then occurs.
The model studies defect evolution through three phases:

- Nucleation: formation of microcracks due to plastic dislocation movement in the metal's crystalline structure. It mainly depends on manufacturing quality. It is assumed that steel used on the GPE line meets the same quality standards as that of the reference line; thus, initial defect probabilities are considered identical.
- Propagation: controlled growth of microcracks to a critical size.
- Failure: rapid, unstable crack growth leading to brittle fracture. This phase is very short, and its influence on X_2 dwell time is negligible. The physical model therefore focuses on the propagation phase, whose duration may differ between lines.

4.3. Assumptions and Development of the Mechanical Model

The model considers the following stresses: vertical bending, horizontal bending in curves, residual rolling stresses (plain rail and welds), Hertzian contact stresses (dependent on elasticity, wheel load, diameter, and contact surface), generating shear

stresses that vary with depth and peak around 5 mm below the surface (Ayel, 2018); Hertzian stresses are assumed to be constant across the tread, since the lateral position of the wheel on the road surface is likely to vary (Profillidis 2000). Furthermore, since the rails are welded at the annual average temperature, stresses related to the temperature gradient are neglected in this study. Similarly, bending stresses in the rail head are also neglected because they are very small.
After defining the constraints, the next step was to determine the forces acting on the rail in a curve. Thus, when the camber is insufficient, centrifugal force generates a lateral force absorbed by the outer rail and an imbalance in the vertical forces on the two rails. There is also a lateral force related to the track contact pattern that acts primarily through the leading axle (on the outer rail). This force exhibits a non-linear evolution and depends on the dynamics of the entire vehicle's (axle, bogie, and body) track engagement in curves. An analytical approximation (Takai et al. 2002), accounting for the friction coefficient and radius, was used for the calculations. Regarding the position of the rail-wheel contact patch on the leading axle in curves, it tends to shift toward the inner flange of the rail. Thus, the tighter the curve, the closer the contact area will be to the inner rail flange. This change in position is also accompanied by a reduction in the contact area, due to the shape of the rail and wheel profiles. This results in an increase in contact stresses. Finally, the contact position in curves may vary very slightly but, at the same time, produce a significant variation in the contact area. In general, the sharper the curve, the greater the variation in lateral forces and stresses caused by even a slight change in the contact position. This phenomenon was simulated numerically for various combinations of vertical and lateral forces (Figure 5), using a semi-Hertzian contact model (Quost et al. 2006). Thus, for given values of the load exerted by the wheel (denoted Q in the figure) and the lateral force absorbed by the rail (denoted Y in the graph), the magnification factor is extrapolated using the curves in this figure and applied to the stresses in Hertz's equation.

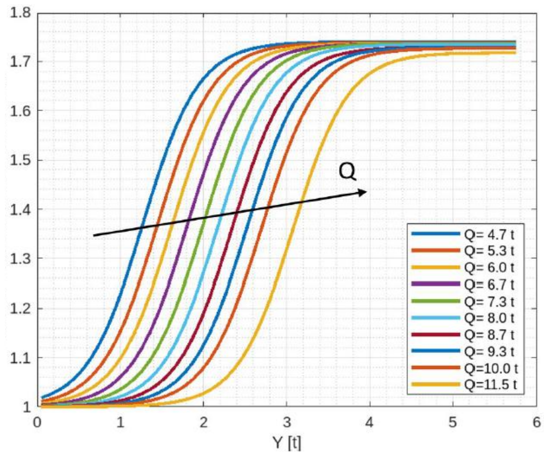

Figure 5: Behaviour of the magnification factor in respect of the lateral force absorbed by the rail (*Y*) for several value of load (*Q*).

The rail is then modelled as a continuous beam supported by the ties. These supports are considered flexible. Referring to the diagram in Figure 2, the maximum vertical bending moment will be equal to:

$$y = \frac{96EI + 14L^3k}{2(96EI + 40L^3k)} QL \qquad (1)$$

Where Q is the vertical wheel load, L is the sleeper spacing, k is the stiffness, I is the moment of inertia of the rail, and E is Young's modulus. The moment increases with the flexibility of the track. This generates compressive stresses in the upper part of the rail, which help slow down the propagation speed of defects. Although the GPE line, considered in this paper (Line 15 south) is laid on a concrete platform, its ties rest on very flexible resilient pads, resulting in a stiffness comparable to that of a ballasted track. The manufacturer provides stiffness values for the simulated track sections ranging from 8 kN/mm to 10 kN/mm. For the reference line (RER Line B), a stiffness of 8 kN/mm was used for all simulations. Vertical and horizontal bending stresses are calculated by treating the rail as a continuous beam on four supports. This is equivalent to considering rail sections resting on four ties. The error introduced by this assumption is relatively small because the efficiency gains between a continuous beam supported on five supports rather than four is negligible. The effect of the stress cycles generated by axle loads moving outside this perimeter is also negligible.

Finally, the dwell times in each considered state (OK, X_1, and X_2) are determined from the defect propagation speed, depending on the difference in stress intensity:

$$\Delta k = Y.K_t.\Delta\sigma.\sqrt{\pi a} \qquad (2)$$

Where $Y = Y_e \cdot Y_{fa} \cdot \underline{Y_s}$ is the correction factor depending on the shape and position of the crack as well as the dimensions of the rail cross-section (Hirt et al. 2006), K_t is the stress concentration factor (a function of the crack width a, generally assumed to be equal to 1), $\Delta\sigma$ is the stress difference induced by a loading cycle at the crack tip, and a is therefore the crack width.

The relationship linking the stress intensity difference to the crack propagation velocity is known as Paris's law, given by:

$$\frac{\mathrm{da}}{dN} = C.(\Delta\mathrm{K})^m \qquad (3)$$

Given N, the number of load cycles, $C = 1.10 \times 10^{-11}$ and $m = 3$ (for steel).

The number of loading cycles required for the crack to grow from size a_i to size a_j is obtained by integrating equation (3) as follows:

$$N_{ij} = \frac{1}{C\alpha\pi^{n/2}Y^m} \cdot \frac{1}{\Delta\sigma^m} \cdot \frac{1}{{a_i}^{\alpha}} \cdot \left(1 - \left(\frac{a_i}{a_j}\right)^{\alpha}\right) \qquad (4)$$

With $\alpha = m/2 - 1$. The number of load cycles is directly related to the number of axles passing over the defect.

It is important to note that the passage of a single axle over a defect can induce multiple load cycles of varying intensities. Equation (4) can still be applied, provided a mathematical convention is used: the equivalent stress difference $\Delta\sigma E$, defined by the following equation. This represents the average stress difference induced by a single load cycle.

$$\Delta\sigma_E = \left(\sum_{i=1}^{k} \Delta{\sigma_i}^m \frac{N_i}{N_{tot}}\right)^{1/m} \qquad (5)$$

Where $\Delta\sigma_i$ is the stress difference induced by load cycle i, N_i is the number of load cycles of type i generated by an axle passing near the defect under study, and N_{tot} is

the total number of load cycles generated by an axle passing near the defect under study.
Finally, for the GPE line considered in this study, simulations were performed with an axle load of 12.5 tons and an average daily tonnage of 81,000 tons. For the reference line (RER B line), annual tonnage values from the RATP's operation database were used. The average number of trains running between each station was estimated using the line's timetables. Static loads are multiplied by an amplification factor to account for dynamic effects, as described in the literature (Ferrara 2013).
This mechanical model thus made it possible to estimate, for different track profiles (straight or with different curve radii), the parameters of the dwell time laws in each of the three rail states considered for the reference line and for the GPE line discussed in this article.
The next section will present the application of this approach to GPE Line 15.

5 Application to Line 15 of the "Grand Paris Express"

Although the study presented in this paper is intended to be extended to the entire future Grand Paris Express network, we illustrate its implementation—and the types of results that can be derived—based on Line 15, linking Noisy-Champs to Pont de Sèvres (Figure 1). To do so, we had the following information available for the RER Line B (the "reference" line) and for Line 15: trackform type, alignments, rail metallurgical characteristics, inventory and positioning of aluminothermic welds, rolling stock characteristics, etc. For Line B, we also had feedback data containing all defect detections, their types, and the histories of preventive and corrective maintenance actions.

5.1. Available Data and Parameterization of the VirMaLab–GPE Tool

The approach presented in Section IV made it possible to obtain Weibull distributions for plain rails and welds, for the different curvature radii considered, and for each rail state transition (OK→X_1, X_1→X_2, and X_2→S). Some of the corresponding cumulative distribution functions are shown in Figure 6.
The next step was to parameterize the VirMaLab framework (Figure 2). The "degradation model" part is obtained from the Weibull laws introduced above. For the rest, the different diagnostic actors as well as the maintenance strategies implemented (condition-based or systematic preventive actions, renewal campaigns, etc.) had to be specified. For rail monitoring, the Grand Paris Express relies on three types of equipment: an ultrasonic inspection vehicle (US), inspecting the track with period T_{US} and able to detect defects X_1 and X_2–S with detection rates respectively denoted τ_1 and τ_2, an onboard video system (VCUB), with inspection period T_{CUB}, detecting the rarer X_2–S defects that have broken through to the surface (i.e., visible externally), walking inspection teams, inspecting the track every T_W , also able of detecting some X_2–S defects.
A representative rail renewal/maintenance strategy also had to be defined. However, since this section aims to illustrate the feasibility and interest of the approach - and because some indicators and parameters are sensitive - some values were adapted here and chosen to remain consistent with the defect propagation laws shown in Figure 6.

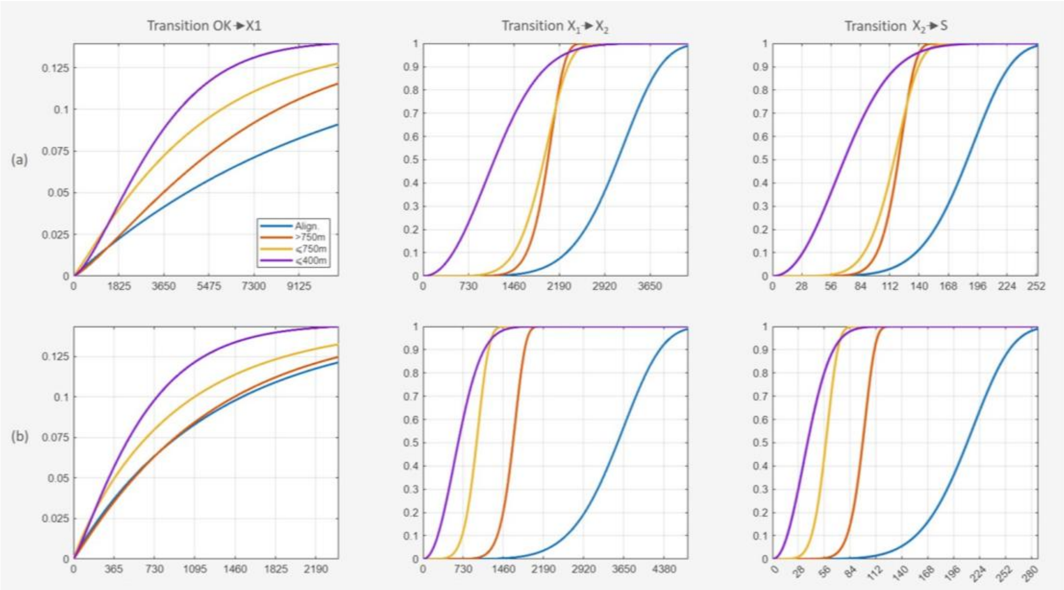

Fig. 6. Weibull Cumulative distribution functions for Line 15 south, derived from the mechanico-statistical approach, representing the time (in days), for different track profiles. (a) Plain rails (b) Aluminothermic welds.

Thus, for these illustrative results (the actual values being confidential), an asset-based renewal of all rails (plain rails and welds) was set to 22 years on tangent track and for sections with curvature radius > 751 m, 12 years for radii < 750 m, 8 years for radii < 400 m. In addition, when a defect (X_1, X_2, or S) is detected, the rail section must be replaced after a given delay, depending on defect type and track geometry. Table I summarizes the selected values. The authors remind the reader that these parameters are provided for illustrative purposes only (while remaining consistent with the sojourn-time laws used) and do not reflect actual operational values.

	Alignment			**Curves, R>400m**			**Curves, *R*≤400m**		
	X_1	**X_2**	**S**	**X_1**	**X_2**	**S**	**X_1**	**X_2**	**S**
Delay (days)	3650	180	1	1460	124	1	183	31	1

Table 1: Replacement delay (days) for different track profiles.

5.2. Sensitivity analysis of US auscultation parameters on X_1 detection delays

In this paper, we proposed to illustrate the use of the considered approach through broken rail prevention management. Indeed, infrastructure managers wanted to evaluate the behavior of X_1 detection delays in respect of different USV strategies and detection rates. Figure 7 introduces these results with the detection delay variation rate, in respect of our reference scenario (black diamond) with T_{US}=183 days and a 60% X_1 detection rate. The variation rates, plotted in figure 7, are given by:

$$\Delta_{T_{US}}^{\tau} = \frac{\mathrm{d}_{T_{US}}^{\tau} - \mathrm{d}_{183}^{60\%}}{\mathrm{d}_{183}^{60\%}} \tag{6}$$

Where *d* denotes the X_1 detection delays estimated by the VirMaLab simulations and τ the X_1 detection rate for the ultrasonic monitoring system.

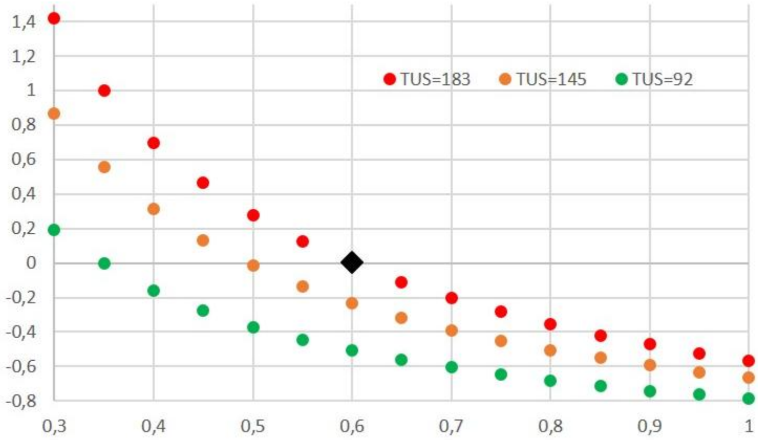

Figure 7: Behaviour of the magnification factor in respect of the lateral force absorbed

First, these simulations help the infrastructure manager to evaluate the impact of the operational X_1 detection rate for the ultrasonic vehicle and predict its maintenance needs for a given monitoring period (among the three ones that are currently discussed for the GPE network). For example, with a 183 days' period, if the detection rate falls to 35%, the detection delay will be doubled whereas, if we want to divide it by two, the detection rate will have to reach 90-95%.

Moreover, considering what is currently the reference strategy (an US auscultation twice a year with a 60% X_1 detection rate), figure 7 also help to understand what could be, at least, the operational detection rate if the infrastructure manager succeeded to survey the tracks more frequently (145 days or 92 days): detection rates could fall, respectively, to 50% and 35%.

4 Conclusions and Contributions

In this paper, we presented an adaptation of the generic VirMaLab approach dedicated to evaluating track monitoring strategies for the Grand Paris Express and preventing rail breaks. Based on the formalism of dynamic Bayesian networks, this approach is typically parameterized using operational feedback data complemented by expert judgment. However, the context of the present study was unique: there is currently no equivalent network (in terms of scale, service frequency, axle load, operating speed, and operational concept) for which long-term rail condition feedback data are available.

To address this limitation, a mechanico-statistical approach was proposed. The first step of this methodology relies on mechanical models of rail defect propagation (under various operating contexts), applied both to the characteristics of the Grand Paris Express lines and to those of a reference line (for this paper, respectively lines 15 and RER B). This comparison made it possible to adapt the sojourn time distributions in the different rail states (for various contexts), known for the reference line, to the specific conditions of the Grand Paris Express. These newly derived distributions were then incorporated into a decision-support tool to evaluate the impact of inspection and maintenance parameters on various indicators.

To illustrate the feasibility and relevance of the proposed approach, a set of simulations was conducted to analyse the impact of ultrasonic vehicle parameters on detection delays for some rail degradations.
Many other scenarios have been considered and simulated in this project. Finally, the aim of this paper was more to present how we dealt with the lack of feedback data proposing the mechanico-statistic approach for a first training of our Bayesian network based decision support tool. This illustrative results will help the readers to understand the interest of such an approach for infrastructure managers when no feedback data are available for standard statistic methods.

References

[1] J. Ayel, Usure dans les moteurs – Formes fondamentales, Techniques de l'ingénieur, 2018, https://doi.org/10.51257/a-v1-bm2753.

[2] L. Bouillaut, O. François, P. Aknin, R. Donat, S. Bondeux, S. Dubois, « VirMaLab — atelier virtuel de maintenance : un outil d'aide à la décision pour l'optimisation des politiques de maintenance ». Recherche Transport et Sécurité, 27, 241-257, 2011, https://doi.org/10.1007/s13547-011-0022-4

[3] L. Bouillaut, O. François, S. Dubois, "A Bayesian network to evaluate underground rails maintenance strategies in an automation context". Proceedings of the Institution of Mechanical Engineers, Journal of Risk and Reliability, 227(4), 411-424, 2013. https://doi.org/10.1177/1748006X134813

[4] L. Bouillaut, O. François, Y. Puttallaz, C. Garnier, C. Cieux, "A hybrid approach for the estimation of rail degradation processes for the Grand Paris new metro", International Journal of Performability Engineering, 16(11), 1685-1697, 2020, https://doi.org/10.23940/ijpe.20.11.p1.16851697

[5] R. Donat, P. Leray, L. Bouillaut, P. Aknin, "Representation of Discrete Duration Models by means of a Specific Dynamic Bayesian Network", Neurocomputing, 73(2), 570-577, 2009, https://doi.org/10.1016/j.neucom.2009.09.012

[6] R. Ferrara, "A numerical model to predict train induced vibrations and dynamic overloads", Phd dissertation, Université Montpellier, 2013.

[7] M.A. Hirt, R. Bez and A. Nussbaumer, "Construction métallique : Notions fondamentales et méthodes de dimensionnement », Traité de Génie civil, 10, 435-491, Presses polytechniques et universitaires romandes, 2006.

[8] R. Lefebre, « Graissage et tribotechnique - Tome 1 : lubrifiants et processus de graissage », Publications de l'Institut français du pétrole, Société des Editions Techniques, 1975.

[9] V.A. Profillidis, Railway Engineering, Second edition, Ed. Ashgate, 2000.

[10] X. Quost, M. Sébès, A. ddhahak, JB. Ayasse, H. Chollet, PE. Gautier, F. Thouverez, « Assessment of a semi-Hertzian method for determination of wheel-rail contact patch". International Journal of Vehicle Mechanics and Mobility, 44(10), 2006, https://doi.org/10.1080/00423110600677948

[11] H. Takai, M. Uchida, H. Muramatsu, H. Ishida, « Derailment Safety Evaluation by Analytic Equations". Quarterly Report of Railway Technical Research Institute, 43(3), 119-124, 2002, https://doi.org/10.2219/rtriqr.43.119